Characteristics of Fine Particle Carbonaceous Aerosol at Two Remote Sites in Central Asia

Justin P. Miller-Schulze[a,b]

Martin Shafer[a,b,*]

James J. Schauer[a,b]

Paul Solomon[c]

Jeffrey Lantz[d]

Maria Artamonova[e]

Boris Chen[f]

Sanjar Imashev[f]

Leonid Sverdlik[f]

Greg Carmichael[g]

Jeff Deminter[a]

a: Wisconsin State Laboratory of Hygiene, 2601 Agriculture Drive, Madison, WI 53718, USA

b: Environmental Chemistry and Technology Program, 660 North Park St, University of Wisconsin, Madison 53706, USA

c: U.S. EPA, Office of Research & Development, Las Vegas, NV 89193 USA

d: U.S. EPA, Office of Radiation and Indoor Air, Las Vegas, NV 89193 USA

e: Institute of Atmospheric Physics, 109017 Moscow, Russia

f: Kyrgyz-Russian Slavic University, 44 Kievskaya Str., Bishkek 720000, Kyrgyz Republic

g: Department of Chemical & Biochemical Engineering, The University of Iowa, Iowa City, IA 52242

*: Corresponding Author:

Email:	mmshafer@wisc.edu
Address:	University of Wisconsin-Madison
	660 N. Park St.
	Madison, WI 53706
Telephone:	608 217 7500
Fax:	608 262 0454

Abstract

Central Asia is a relatively understudied region of the world in terms of characterizing ambient particulate matter (PM) and quantifying source impacts of PM at receptor locations, although it is speculated to have an important role as a source region for long-range transport of PM to Eastern Asia, the Pacific Ocean, and the Western United States. PM is of significant interest not only because of its adverse effect on public health but also due to its more recently realized role in climate change. To investigate the sources and characteristics of PM in the region, a series of $PM_{2.5}$ and PM_{10} samples were collected on an every-other-day basis at two sites (termed "Bishkek" and "LIDAR") in the Central Asian nation of the Kyrgyz Republic (also known as Kyrgyzstan) for a full year from July 2008 to July 2009. These samples were analyzed using standard methods for mass, organic carbon (OC), elemental carbon (EC), water-soluble organic carbon (WSOC), water-insoluble organic carbon by difference (OC minus WSOC) and a variety of molecular marker chemical species to be used in a chemical mass balance (CMB) model to apportion the sources of OC. These analyses indicate that approximately 19 ± 6.4 % of the $PM_{2.5}$ mass at both sites throughout the year consists of OC. The carbonaceous component of $PM_{2.5}$ is dominated by OC, with OC/Total Carbon (TC) ratios being around 0.8 in the winter to almost 0.95 in the summer months. The CMB analysis indicated that mobile sources, i.e., gasoline and diesel engine exhaust, biomass combustion, and biogenic secondary organic aerosol (SOA) formation from isoprene and α-pinene precursors in the summer months were the dominant sources of OC. A strong positive correlation was observed between non-biomass burning WSOC and the un-apportioned OC from the CMB analysis, indicating that some of this un-apportioned OC is WSOC and likely the result of SOA-forming atmospheric processes that were not estimated by the CMB analysis performed. In addition, a comparison of the predominant contributors to OC between the two sites indicates that biomass combustion is a stronger relative source of OC at the LIDAR site, particularly in the winter, while contributions of isoprene- and α-pinene-derived SOA to the measured OC was relatively similar between the sites.

1. Introduction

The impact on climate of atmospheric aerosol is dependent on the chemical and physical characteristics of the aerosol; as these characteristics affect the aerosol's lifetime, interaction with light, and influence on cloud formation. Carbonaceous aerosols are a significant contributor to PM concentrations around the world (Davidson, Phalen et al. 2005, Solomon and Costa 2010). These aerosols are of great interest to the scientific community due to their role in radiative forcing and, subsequently, both global and regional climate change (Haywood and Boucher 2000), as well as due to their adverse effect on human health (Davidson, Phalen et al. 2005).

However, there currently is a lack of data on carbonaceous aerosol levels and chemical speciation for a number of areas around the world, reflecting both the difficulties in PM sampling in remote regions and the relatively sophisticated analytical protocols required for speciation. A number of approaches have been employed to fill in these data gaps, including an assortment of PM/carbonaceous aerosol modeling studies (Cooke and Wilson 1996; Chung and Seinfeld 2002), as well as estimations of global organic carbon (OC) and black carbon (BC) based on fuel consumption data (Bond, Streets et al. 2004). However, as with all modeling studies, accurately predicting the concentrations at sites where the regional influences are not well-characterized is challenging. For example, a 2002 study (Chung and Seinfeld 2002) used the Goddard Institute for Space Studies Global Circulation Model II-Prime to model OC and BC concentrations for a variety of types of sampling sites around the world. The authors found that the model consistently underestimated both OC and BC at all sampling sites, which they hypothesize resulted from an underestimation of OC and BC emissions in the model input and/or an overestimation of wet scavenging by clouds.

Our understanding of the role of aerosols in processes that affect climate (and, consequently, the policy actions taken regarding these aerosols) is based on our knowledge of their chemical and physical characteristics. This understanding is, in many cases, based on our ability to incorporate aerosol effects into climate models. The chemical and physical characteristics of aerosols are necessarily a function of their source. For example, biomass combustion produces OC that is predominantly water-soluble (Sannigrahi, Sullivan et al. 2006), whereas diesel fuel combustion produces relatively less water-soluble OC (Cheung, Polidori et al. 2009), due to differences in fuel type and combustion temperature. Processes affecting climate, such as cloud formation, will be affected differently by aerosols from these two sources. The effect of chemical characteristics of aerosols on cloud formation, aerosol lifetime, and regional transport illustrates the importance of understanding the sources of atmospheric aerosol. While emissions inventories based on fuel consumption data have been employed for this purpose, as noted above, these inventories potentially exclude the contributions to atmospheric PM by sources that are not well estimated from fuel usage, such as secondary organic aerosol and other primary non-combustion sources. As such, detailed measurements and source apportionment of aerosols in understudied regions is an important first step in establishing the relevant chemical characteristics and sources of PM; this knowledge can then be applied to existing and future modeling studies to constrain model inputs and evaluate the performance of model outputs.

Central Asia is one of the areas for which very little detailed chemical data on ambient PM exists. However, recent work suggests that East-Central Asia may be an important source region for PM involved in long-range transport to, for example, the U.S. (Fischer, Hsu et al. 2009) . The Gobi and Taklamakan Deserts in western China and Mongolia are thought to be the source of much of this transported PM (Fischer, Hsu et al. 2009), though aerosol from the Aral Sea region in Central Asia is also likely contributing. The volume of the Aral Sea has decreased markedly over the last half-century, due to intensive irrigation using waters from the feeder rivers, and as a result, parts of the Aral Sea region have been transformed into an open salt desert (Singer, Zobeck et al. 2003). This has resulted in an increased frequency of dust storms in the region (O'Hara, Wiggs et al. 2000), events that could influence the areas further east of the Aral Sea and supplement other major dust sources. Because of the lack of data on the chemical characteristics of the PM in Central Asia, it is unclear what the impact of dust storms originating from the Aral Sea zone and other PM source regions in Central Asia are on both regional and global levels of PM.

The data presented in this manuscript is one component of a larger project comprised of a full year of every-other-day PM sampling that was conducted at two sites in the Kyrgyz Republic (also known as Kyrgyzstan) from mid-July 2008 through mid-July 2009. The overarching goal of the study was to obtain a detailed chemical characterization of the ambient PM collected in the Kyrgyz Republic during the sampling period and to estimate the contribution of the sources of this aerosol to the regional and transcontinental flow of PM. Results presented here focus on the carbonaceous components of the collected PM, and the resulting chemical mass balance (CMB) analysis of the OC fraction to investigate the sources of this component of the aerosol.

2. Experimental

2.1. Description of Sampling Region

The Kyrgyz Republic is bordered by China to the east, Kazakhstan to the north, Uzbekistan to the west, and Tajikistan to the south. The Aral Sea region lies 1200 km to the west. The terrain in the Kyrgyz Republic is quite mountainous, and the majority of the population lives in rural areas (65%). The total population of the country as of 2008 is approximately 5.4 million with a significant fraction (approximately 825000 as of 2009) living in the largest city and capital of the country, Bishkek (http://www.placesdata.com/world/kyrgyzstan/bishkek/). The location of the Kyrgyz Republic in Central Asia is shown in Figure 1. Although a detailed emissions inventory was not available for this study, our knowledge of the region suggests that most electricity is generated by hydroelectric power plants. Coal-fueled electropower stations are used in urban areas to produce hot water for residential heating, whereas in more rural areas, heat is produced by a combination of electricity, residential coal stoves, and wood and dung (i.e., biomass) combustion.

2.2. Sample Collection and Filter Compositing

PM samples (24 hour) were collected at the two sampling sites, Bishkek and LIDAR, from mid-July 2008 to mid-July 2009 on an every-other-day basis. The approximate locations of the sampling sites are shown in Figure 1. The Bishkek sampling site was located 23 km south of the Bishkek city center, at 42°

40’ 47.80” N, 74° 31’ 44.30” E. The LIDAR sampling site (so named due to a LIDAR instrument being present at the site) was 11 km east and slightly south of the city center of Karakol, population ~70000 (http://placesdata.com/world/kyrgyzstan/karakol/), at an elevation of 1920 m at 42° 27’ 49.30” N, 78° 31’ 49.30” E. The closest city, 3.7 km directly north of sampling site, was Teploklyuchenka, population ~9000, (http://placesdata.com/world/kyrgyzstan/teploklyuchenka/). The population within 35 km of Teploklyuchenka is about 162,000 (http://placesdata.com/world/kyrgyzstan/teploklyuchenka/). Both sampling sites are in mountain ranges with valleys to the north and essentially no population to the south, with mountains that reach elevations greater than 3500 m above sea level (ASL) south of the Bishkek site and 4600 m ASL south of the LIDAR site. The distance between the two sampling sites was approximately 315 km direct.

At each site on each sampling day, eight samples were collected using URG 3000ABC samplers (URG Corporation, U.S.A.): 2 PM_{10} samples on quartz filters, 2 PM_{10} samples on Teflon filters, 2 $PM_{2.5}$ samples on quartz filters and 2 $PM_{2.5}$ samples on Teflon filters. Teflon and quartz-fiber filters were obtained from VWR (VWR International, U.S.A.). Prior to use, the quartz-fiber filters were baked at 550 °C for a minimum of 12 hr. Teflon filters were equilibrated for 24 hr prior to use as described below (section 2.3). As needed based on method detection limits, filters or filter portions were composited into bi-weekly or monthly sample composites. One section (1.5 cm^2) of one of the $PM_{2.5}$ quartz-fiber filters was analyzed for EC and OC, whereas a second punch was taken from this quartz filter and analyzed for water-soluble organic carbon (WSOC). The remaining portion of the quartz-fiber filters along with the other co-collected $PM_{2.5}$ quartz filter from that sampling day were collected into monthly composites to quantify specific organic molecular markers typically employed in CMB analysis. In each monthly composite, approximately 1.5 filters from each sampling day were included, totaling approximately 22.5 filters in each composite, representing a sampled volume of approximately 266 m^3.

2.3. Chemical Analysis

The mass of the PM samples was determined gravimetrically using a high-precision microbalance (MX5, Mettler-Toledo, U.S.A) with 1 µg readability. Teflon filters were tared and post-weighed in a temperature (21 ± 2 °C) and humidity (35 ± 3% RH) controlled weighing room, and equilibrated in the room for a minimum of 18 hours before weighing. Any static charge on the filters was eliminated with a Po-ionization source. The total uncertainty associated with the mass measurement was <7% or +/- 4 µg (which ever was greater).

EC and OC concentrations were determined with a thermal-optical EC/OC analyzer (Sunset Laboratories, U.S.A.) and using the ACE-Asia base-case protocol (Schauer, Mader et al. 2003). Explicit details of this analysis protocol can be found in the supporting information (SI).

WSOC was determined using the method outlined in Snyder, et al. (2009). In this method, bi-weekly composites of the quartz-fiber filter sections (1.5 cm^2) were extracted in 12 ml of water, and the solubilized OC was quantified with a Sievers 900 TOC analyzer (GE Analytical, U.S.A.). The accuracy of the WSOC method for this data set, as determined by the average % recovery ± standard deviation of standard mixtures of KHP (potassium hydrogen phthalate) was 108 ± 9%. All samples were laboratory

169 blank and subsequently field blank subtracted to correct for WSOC contamination of filters, glassware,
170 reagents, etc. Both blank subtractions were done on an extract-concentration basis, using the method
171 blanks from the relevant analysis sequence and the overall average of the field blanks. The average level
172 of WSOC blank contamination in the field blanks was 0.34 ± 0.04 $\mu g/m^3$.

173 Water-insoluble organic carbon (WIOC) was calculated as the difference between OC and WSOC as
174 determined by the aforementioned methods.

175 The organic species employed as molecular markers/chemical tracers were determined from monthly
176 composites of the quartz-fiber filters minus the two 1.5 cm^2 sections noted above (for WSOC and OC
177 analysis). The extraction and gas chromatography-mass spectrometry (GC-MS) method has been
178 detailed in a previous publication (Stone, Snyder et al. 2008), but will be described briefly here. This
179 extraction and GC-MS method involved spiking the composite samples with isotopically-labeled
180 standard solutions for quantification purposes and subsequent Soxhlet extraction with dichloromethane
181 and methanol in sequence. The extracts were then concentrated by rotary evaporation and further
182 evaporated under purified nitrogen gas to a final volume of 250 µl. These extracts were then analyzed
183 by GC-MS (GC: 6890, MS: 5973, column: DB-5 capillary column; Agilent Technologies, U.S.A.), once after
184 derivitization of the carboxylic acid functionalities with azomethane, and again after the silylation of the
185 hydroxyl groups (Nolte, Schauer et al. 2002). All analytes for all sample composites were field-blank
186 subtracted to address any contamination of filters, filter-cutting equipment, and other laboratory
187 equipment.

188 The calculated uncertainty of the air concentrations of all analytes represents the <u>greater</u> of the square
189 root of the sum of the squares of a) the standard deviation of the analyte concentration present in the
190 field blanks and a 20% of the calculated analyte concentration in the composite "correction" factor or b)
191 ½ the value of the limit of detection for that analyte and the 20% "correction" factor. Further details of
192 the GC-MS method and calculations can be found in the aforementioned publication by Stone, et al.
193 (Stone, Snyder et al. 2008).

194 *2.4. Source Apportionment using Chemical Mass Balance*

195 The sources of the OC fraction of $PM_{2.5}$ were apportioned using CMB software developed by the U.S.
196 Environmental Protection Agency (EPA), the current version of which is publically available (EPA CMB
197 v8.2). The CMB program solves for an effective-variance least-squares solution to the linear combination
198 of the product of the source contribution and its concentration (Watson, Cooper et al. 1984). Tables 1A
199 and 1B list the molecular marker compounds that were employed as fitting (tracer) species for the CMB
200 analysis, along with the minimum and maximum concentrations observed in the composite samples and
201 the relevant source profiles for each tracer. Molecular marker species employed in this analysis were
202 assumed to be stable during transport from source to receptor.

203 The source profiles used in the optimized analysis (as described below) for both sites are as follows:
204 Georgia Open Burn/Biomass Burning (Lee, Baumann et al. 2005); Natural Gas Combustion (Rogge,
205 Hildemann et al. 1993); Diesel Exhaust (Lough, Christensen et al. 2007); Gasoline Engines (Lough,
206 Christensen et al. 2007); Smoking Gasoline Vehicles (Lough, Christensen et al. 2007); Residential (low

temperature) Bituminous Coal Combustion (Zhang, Schauer et al. 2008); α-Pinene- and Isoprene-Derived SOA (Lewandowski, Jaoui et al. 2007).

In order to apportion the OC derived from Secondary Organic Aerosol (SOA) formation, tracer species were employed as per Kleindienst, et al. and Stone, et al. (Kleindienst, Jaoui et al. 2007, Stone, Snyder, et al. 2009). It should be noted that the OC apportioned to SOA formation from α-pinene and isoprene precursors using the CMB analysis should not be interpreted as being an estimation of the total OC from all SOA formation processes. Rather, the OC apportioned to SOA from α-pinene and isoprene precursors is an estimation of a subset of the OC from SOA derived from specific precursor species.

The choice of the source profiles employed in the CMB analysis was based on existing knowledge of the region and subsequent sensitivity/error analysis as described in previous studies (Sheesley, Schauer et al. 2007). The selection of the Georgia Open Burn profile to represent biomass combustion in the study region(s) was motivated by the assumption that the fuel was comprised of less hardwood-type wood and more soft woods and grasses. With regards to the mobile source profiles (i.e., gasoline vehicle and diesel exhaust), an analysis of the standard error (S.E.) of the source contribution estimates (SCEs) in the CMB output suggested that the contribution of mobile sources to OC levels could be approximated through the use of two profiles ("Smoking" Gasoline Vehicles and Diesel Exhaust) as opposed to three ("Smoking" Gasoline vehicles, "Non-Smoking" Gasoline Vehicles and Diesel Exhaust). "Smoking" Gasoline Vehicles are defined as vehicles that either release visible amounts of smoke or emit greater than 50 mg EC/mile (Lough, Christensen et al. 2007). In addition, the error in the calculated reconstruction of the molecular marker concentrations using the two-profile option was less than the error using the three-profile option. The sum of the SCEs for the three-profile method also was found to be not statistically different from the sum of the SCEs for the two-profile method. These results are consistent with the lack of motor vehicle emissions controls in the Kyrgyz Republic. The implication of this for this study is that the OC emissions for all gasoline vehicles relevant to the two sampling sites were approximated by the "Smoking" Gasoline Vehicle source profile established by Lough, et al. A previous publication from our laboratory employed similar approach to estimate total gasoline engine emissions (catalyzed, non-catalyzed, and two-stroke) using a single profile (non-catalyzed gasoline engines) in the CMB analysis of aerosol collected in Lahore, Pakistan (Stone, Schauer, et al. 2010).

3. Results and Discussion

3.1. Particulate Matter Levels and Organic Carbon Contribution

The $PM_{2.5}$ OC and percent OC in $PM_{2.5}$ observed at each sampling site are presented as monthly averages in Table 2. The uncertainties shown represent the standard error (i.e., standard deviation in the PM concentration measurements for the month divided by the square root of the number of PM measurements in that month).

The $PM_{2.5}$ concentrations are similar between the two sites and exhibit similar trends from month to month. Higher $PM_{2.5}$ levels are observed in the summer as compared with the winter at both sites, and particularly at the Bishkek site, where the difference is about 30%. Between the two sites, higher

concentrations are observed at Bishkek in the fall (~30% on average) whereas in the winter higher concentrations (~20% on average) are observed at the LIDAR site.

The average contribution of OC to $PM_{2.5}$ is between 12 and 23% at the Bishkek site and 11 and 38% at the LIDAR site, with the higher contributions (approximately a factor of 2 on average) occurring during the winter months at the LIDAR site. On an annual average basis, OC contributes about 20% to $PM_{2.5}$ at both sites, indicating the importance of identifying and quantifying the sources of OC to better understand the dynamics of PM in the region.

3.2. Chemical Characteristics of Carbonaceous Aerosol

The monthly average OC and EC concentrations, measured at the two sampling sites are shown in Figures 2A-2D. Total OC is further split into WSOC and WIOC. For reference, the monthly average $PM_{2.5}$ concentration data is also shown in Figures 2A and 2B. The ratio of OC to total carbon (TC), which is the sum of the OC and EC concentrations, is presented for both sites in Figures 2C and 2D. An alternate presentation of the OC/TC data, in the form of the OC/EC ratio, is presented in the SI.

The predominant sources of WSOC include biomass burning and secondary organic aerosol (SOA) formation, from natural and anthropogenic precursors (Snyder, Rutter et al. 2009). The majority of OC in biomass burning emissions are in the form of WSOC (Sannigrahi, Sullivan et al. 2006; Snyder, Rutter et al. 2009), with the remainder being WIOC (by difference). Another source of WIOC is fossil fuel combustion. Sources of EC include diesel exhaust, coal combustion, and biomass burning (Schauer 2003).

The distinctive and similar trend in the monthly average OC/TC ratios at the two sampling sites is striking. At both sites, a “U” shaped pattern is observed, with the highest OC/TC values observed during the summer months and the lowest OC/TC values observed in the winter months. The increase in EC relative to TC can likely be attributed to increased diesel fuel combustion (either in diesel vehicles or in diesel fuel oil heating furnaces) and the increase in coal combustion in the winter months. Increased levels of EC appears be driving the decreasing OC/TC ratio in the winter months at the LIDAR site. At the Bishkek site, increased levels of EC are also observed during the winter months; however, the increase in the OC/TC ratio in the summer seems to be driven more by an increase in OC, and more specifically, WSOC, than a decrease in EC. The source of the increased WSOC at Bishkek in the summer months is not apparent from the collected data.

One apparent “outlier” in the U-shaped trend of the OC/TC ratio described above is the OC/TC value for January 2009 at the Bishkek site. Examination of Figure 2A shows that the EC and $PM_{2.5}$ levels are low in comparison with the other winter months at Bishkek. While the OC is also low relative to these adjacent months, it is not as low as the EC proportionally, leading to the observed relatively higher OC/TC ratio. One possible cause of this high OC/TC value and low $PM_{2.5}$ value is a boundary layer preventing mixing of local air with air transported from relatively further afield of the sampling site (and that this transported air has a relatively higher concentration of EC). However, examination of basic meteorological data for the winter months in Bishkek does not indicate these types of atmospheric conditions, and further in-

depth meteorological analysis is beyond the scope of this paper. As such, the reason for this relatively high OC/TC value in January 2009 at Bishkek is not clear.

3.3 Source Apportionment of Organic Carbon

The numeric output of the CMB analysis used for source apportionment of OC at the Bishkek and LIDAR sites is presented in Tables 3 and 4, respectively. In addition, the percent of total monthly average OC represented by each SCE is given in Tables SI-2A and SI-2B of the SI. The "Smoking" Gasoline Vehicle and Diesel Exhaust SCEs are summed and presented as Mobile Sources and the Isoprene-derived and α-Pinene-derived SCEs are summed as Biogenic SOA, as these SCEs were observed to vary together and result from similar processes/activities. Tables of CMB analytical diagnostic values (i.e., % mass apportioned, χ^2, r^2) are presented in the SI. Figures 3A and 3B present the CMB SCEs graphically; with the "Smoking" Gasoline Vehicle and Diesel Exhaust SCEs as well as Isoprene- and α-Pinene-derived SOA SCEs shown individually.

As Tables 3 and 4 and Figures 3A and 3B (and the tables in the SI) show, the results of the CMB analysis indicate that at both sites, Mobile Sources (Bishkek: 10%-52%, LIDAR: 13%-46%) and Biomass Burning (Bishkek: 2%-16%, LIDAR: 8%-33%) account for up to 60% and 67% of the apportioned OC mass in a given month at Bishkek and LIDAR, respectively. In addition, OC resulting from α-Pinene- and Isoprene-derived SOA formation is significant in the summer months, accounting for greater than 10% up to 17% of the OC at the Bishkek site and up to 38% of the OC at the LIDAR site. Natural Gas was determined to be a consistent but relatively minor source (<2%) of OC at both sampling sites (with higher contributions in the winter months). Low-Temperature Coal Combustion also was a minor (<3%) source of OC in the winter months. At the Bishkek site, the portion of OC mass from un-apportioned sources was relatively higher in the summer months, while at the LIDAR site, the un-apportioned OC mass did not show clear patterns. Overall, between 18%-62% of OC was apportioned at the Bishkek site and between 32%-85% at the LIDAR site. The higher fraction apportioned at the LIDAR site was likely due to the greater impact of sources attributed to the Biomass Burning profile in the winter since the other apportioned sources contributed more evenly at each of the sites. For reference, recent CMB studies in Lahore, Pakistan have apportioned between 55 and 100% of the monthly average OC (Stone, Schauer, et al. 2010), and between 37 and 54% of annual average OC in numerous countries in the Middle East (von Schneidemesser, Zhou et al. 2010).

Figures 3A and 3B and Tables 3 and 4 show that a significant amount of the OC was not apportioned (i.e., "CMB Other") at both sites for the entire sampling period. While the source profiles employed for this analysis included two SOA profiles (α-Pinene- and Isoprene-derived SOA), it is still likely that SOA not apportioned by these CMB source profiles is a significant contributor to the measured OC. Hypotheses along these lines have been discussed in several other recent studies (Sheesley, Schauer et al. 2004; Stone, Snyder et al. 2008; Lin, Lee et al. 2010). Most SOA that is OC is water-soluble, due to its oxygenated character (Stone, Snyder et al. 2008). The 2009 study by Snyder, et al. found that non-biomass WSOC was highly correlated with CMB "Other" in their study of carbonaceous aerosol from the midwestern United States. As such, the relationship between WSOC and CMB Other is informative in

this context, i.e., as a second method of estimating the contribution of SOA to OC. The relationship between WSOC and CMB Other is presented for both sites in Figures 4A and 4B.

As seen in Figures 4A and 4B, there is a strong positive correlation between WSOC that calculated to be not derived from biomass combustion and the sum of the CMB Other and α-Pinene- and Isoprene-derived SOA at both sites. The fraction of WSOC not derived from combustion of biomass was estimated using the ratio employed by Snyder, et al. (Sannigrahi, Sullivan et al. 2006; Snyder, Rutter et al. 2009). The SCEs from the two SOA profiles employed in the CMB analysis were added to the CMB Other SCE since it was not possible to differentiate the OC from α-pinene and isoprene precursors and the OC from other SOA precursors, both of which would be represented as non-biomass WSOC on the x-axis of Figures 4A and 4B.

One interpretation of this positive correlation is that the un-apportioned OC consists of SOA, made of up WSOC. However, the regression slopes in Figures 4A and 4B are both >1, indicating that this hypotheses does not fully explain the un-apportioned OC. The remainder of this un-apportioned OC, then, could be (a) the product of SOA that is not WSOC, (b) from processes that were not included in the CMB analysis (i.e., sources of OC not described by the source profiles employed, for example, vegetative detritus), or (c) underestimation of the OC produced by a source for which a profile was used. The remainder of this un-apportioned OC could not be further apportioned based on the available data.

3.4. Comparison of Carbonaceous Aerosol Sources between Sampling Sites

The measured EC at the two sampling sites is possibly the result of different processes. At the Bishkek site, it is reasonable to expect that the coal-burning electropower stations in the region are likely to contribute significantly to ambient EC. In the region represented by the LIDAR site, where these types of central electropower stations for residential heat are less common or not present, the EC is most likely the result of low-temperature coal combustion in residential coal stoves and wood (i.e., biomass) burning for residential heating purposes. The relative prevalence of residential coal combustion is evident from the CMB analysis (shown graphically in the SI), which shows a higher amount of OC apportioned to low-temperature coal combustion at the LIDAR site during the winter months as compared with the Bishkek site.

In order to examine the differences in OC levels and sources between the two sites, the monthly average of the measured OC as well as the SCEs from the CMB analysis for the Biogenic SOAs, Biomass Burning, and Mobile Sources at the two sites were plotted in Figures 5A-5D, respectively. In addition, a comparison of the monthly averages for WIOC, WSOC, and EC are presented in the SI.

The monthly average OC values (Figure 5A) are fairly evenly distributed on both sides of the 1/1 line. However, there is a seasonal dependence to the distribution. In the summer, higher levels of OC were observed at the Bishkek site as compared with the LIDAR site, and vice-versa for winter. In terms of the higher average levels of OC at the LIDAR site in the winter, this can be explained in part by contrasts in the Biomass Burning-derived OC (Figure 5C) and Mobile Source-derived OC (Figure 5D), respectively, at the two sampling sites. In the winter (Figure 5C), the average OC levels from biomass combustion are approximately 3-10 times greater at the LIDAR, which is in agreement with our expectations of the

relevant sources likely impacting the two sites. Increased levels of OC are also attributed to Mobile Sources at the LIDAR site as compared to the Bishkek site for the winter months, as shown in Figure 5D, although to a lesser extent as compared with the OC attributed to Biomass Burning.

The reason behind the higher monthly averages for OC at the Bishkek site in the summer is less clear than the effect discussed previously for winter at the LIDAR site. One possibility is that greater amounts of SOA are produced at the Bishkek site in the summer, however, as Figure 5B indicates, the SOA-derived contribution to OC from α-pinene and isoprene precursors is more or less the same at both sampling sites. It is possible that SOA formation not represented by the α-pinene and isoprene precursor source profiles is contributing. The increased WSOC levels observed at Bishkek in the summer supports this hypothesis (Figure 2A, SI).

4. Conclusion

The results of our analysis of $PM_{2.5}$ collected at two sites in the Kyrgyz Republic from July 2008 until July 2009 indicate that OC is an important (~20%) contributor to $PM_{2.5}$ in the region. The carbonaceous component of $PM_{2.5}$ was observed to be mostly OC, with relatively greater amounts of EC observed in the winter and higher levels of OC observed at the Bishkek site in the summer and LIDAR site in the winter. The results of our CMB analysis indicate that mobile sources, consisting of diesel and gasoline engine emissions, comprised the bulk of the primary source emissions at both sites. Biomass combustion was also found to be a significant contributor to OC at both sites, particularly in the winter months. SOA was identified as an important source of OC, but only in the summer months, and to a greater extent at the LIDAR site as compared with the Bishkek site.

A strong linear correlation was observed between the non-Biomass Burning WSOC and the sum of the un-apportioned OC (i.e., CMB "Other") and biogenic SOA OC, indicating that the source for OC defined as CMB "Other" is quite possibly SOA formation pathways in which isoprene and/or α-pinene are not precursor species. A comparison of the CMB SCEs from the two sites indicates that biomass combustion is a more significant contributor to OC at the LIDAR site in the winter months, whereas the un-apportioned OC levels were much higher at the Bishkek site in the summer, suggesting a more significant impact from this type of SOA (i.e., non-isoprene or α-pinene derived) at Bishkek.

The data presented in this manuscript substantively contributes our knowledge-base of $PM_{2.5}$ sources and relative levels of OC and EC for an understudied region of the world, i.e., Central Asia. Although the results described in this manuscript may not necessarily be used directly in climate models, the results in terms of relevant sources of OC and $PM_{2.5}$ and levels of OC, EC and WSOC can be used to fill in data gaps about which processes are important to the carbonaceous aerosol concentrations and characteristics in this region. In addition, characterizing the sources of OC and $PM_{2.5}$ at these sites will facilitate our subsequent investigation into the relevance of wind-blown dust from the Aral Sea to the regional PM concentrations as well as to the contribution of PM from Central Asia to global PM levels.

Acknowledgements

Justin P. Miller-Schulze would like to acknowledge the Association of Public Health Laboratories (APHL) for funding through their Environmental Health Fellows program. The authors would also like to acknowledge Brandon Shelton and Erin Mani at the Wisconsin State Laboratory of Hygiene for their efforts with the molecular marker and WSOC analysis, respectively. The US Environmental Protection Agency through its Office of Research and Development funded this study and collaborated in the research described here under Contract EP-D-06-001 to the University of Wisconsin-Madison) as a component of the International Science & Technology Center (ISTC) project # 3715 (Transcontinental Transport of Air Pollution from Central Asia to the US). It has been subjected to Agency review and approved for publication.

References

Bond, T. C., D. G. Streets, et al. (2004). "A technology-based global inventory of black and organic carbon emissions from combustion." Journal of Geophysical Research-Atmospheres **109**(D14).

Cheung, K. L., A. Polidori, et al. (2009). "Chemical Characteristics and Oxidative Potential of Particulate Matter Emissions from Gasoline, Diesel, and Biodiesel Cars." Environmental Science & Technology **43**(16): 6334-6340.

Chung, S. H. and J. H. Seinfeld (2002). "Global distribution and climate forcing of carbonaceous aerosols." Journal of Geophysical Research-Atmospheres **107**(D19).

Cooke, W. F. and J. J. N. Wilson (1996). "A global black carbon aerosol model." Journal of Geophysical Research-Atmospheres **101**(D14): 19395-19409.

Davidson, C. I., R. F. Phalen, et al. (2005). "Airborne particulate matter and human health: A review." Aerosol Science and Technology **39**(8): 737-749.

Fischer, E. V., N. C. Hsu, et al. (2009). "A decade of dust: Asian dust and springtime aerosol load in the US Pacific Northwest." Geophysical Research Letters **36**.

Haywood, J. and O. Boucher (2000). "Estimates of the direct and indirect radiative forcing due to tropospheric aerosols: A review." Reviews of Geophysics **38**(4): 513-543.

Kleindienst, T. E., M. Jaoui, et al. (2007). "Estimates of the contributions of biogenic and anthropogenic hydrocarbons to secondary organic aerosol at a southeastern US location." Atmospheric Environment **41**(37): 8288-8300.

Lee, S., K. Baumann, et al. (2005). "Gaseous and particulate emissions from prescribed burning in Georgia." Environmental Science & Technology **39**(23): 9049-9056.

Lewandowski, M., M. Jaoui, et al. (2007). "Composition of PM2.5 during the summer of 2003 in Research Triangle Park, North Carolina." Atmospheric Environment **41**(19): 4073-4083.

Lin, L., M. L. Lee, et al. (2010). "Review of Recent Advances in Detection of Organic Markers in Fine Particulate Matter and Their Use for Source Apportionment." Journal of the Air & Waste Management Association **60**(1): 3-25.

Lough, G. C., C. G. Christensen, et al. (2007). "Development of molecular marker source profiles for emissions from on-road gasoline and diesel vehicle fleets." Journal of the Air & Waste Management Association **57**(10): 1190-1199.

Nolte, C. G., J. J. Schauer, et al. (2002). "Trimethylsilyl derivatives of organic compounds in source samples and in atmospheric fine particulate matter." Environmental Science & Technology **36**(20): 4273-4281.

O'Hara, S. L., G. F. S. Wiggs, et al. (2000). "Exposure to airborne dust contaminated with pesticide in the Aral Sea region." Lancet **355**(9204): 627-628.

Rogge, W. F., L. M. Hildemann, et al. (1993). "Sources of Fine Organic Aerosol .5. Natural-Gas Home Appliances." Environmental Science & Technology **27**(13): 2736-2744.

Sannigrahi, P., A. P. Sullivan, et al. (2006). "Characterization of water-soluble organic carbon in urban atmospheric aerosols using solid-state C-13 NMR spectroscopy." Environmental Science & Technology **40**(3): 666-672.

Schauer, J. J. (2003). "Evaluation of elemental carbon as a marker for diesel particulate matter." Journal of Exposure Analysis and Environmental Epidemiology **13**(6): 443-453.

Schauer, J. J., B. T. Mader, et al. (2003). "ACE-Asia intercomparison of a thermal-optical method for the determination of particle-phase organic and elemental carbon." Environmental Science & Technology **37**(5): 993-1001.

Sheesley, R. J., J. J. Schauer, et al. (2004). "Trends in secondary organic aerosol at a remote site in Michigan's upper peninsula." Environmental Science & Technology **38**(24): 6491-6500.

Sheesley, R. J., J. J. Schauer, et al. (2007). "Sensitivity of molecular marker-based CMB models to biomass burning source profiles." Atmospheric Environment **41**(39): 9050-9063.

Singer, A., T. Zobeck, et al. (2003). "The PM10 and PM2.5 dust generation potential of soils/sediments in the Southern Aral Sea Basin, Uzbekistan." Journal of Arid Environments **54**(4): 705-728.

Snyder, D. C., A. P. Rutter, et al. (2009). "Insights into the Origin of Water Soluble Organic Carbon in Atmospheric Fine Particulate Matter." Aerosol Science and Technology **42**(11): 1099-1107.

Stone, E. A., D. C. Snyder, et al. (2008). "Source apportionment of fine organic aerosol in Mexico City during the MILAGRO experiment 2006." Atmospheric Chemistry and Physics **8**(5): 1249-1259.

Stone, E.A., Zhou, J., et al. (2009). "A Comparison of Summertime Secondary Organic Aerosol Source Contributions at Contrasting Urban Locations." Environmental Science and Technology **43**(10): 3448-3454.

Stone, E. A., J. J. Schauer, et al. (2010) "Chemical characterization and source apportionment of fine and coarse particulate matter in Lahore, Pakistan" Atmospheric Environment **44**(8): 1062-1070.

Solomon, P.A. and D.L. Costa (2010). Ambient tropospheric particles. In: Gehr P, Rothen-Muhlfeld B, Blank F. (eds) Particle-lung Interactions, 2nd eds. Informa Healthcare, New York, pp 17-37.

United Nations (2003). World Statistics Pocketbook Landlocked Developing Countries**:** 25.

von Schneidemesser, E., J. Zhou, et al. (2010) "Seasonal and spatial trends in the sources of fine particle organic carbon in Israel, Jordan, and Palestine" Atmospheric Environment **44**(30): 3669-3678.

Watson, J. G., J. A. Cooper, et al. (1984). "The Effective Variance Weighting for Least-Squares Calculations Applied to the Mass Balance Receptor Model." Atmospheric Environment **18**(7): 1347-1355.

Zhang, Y. X., J. J. Schauer, et al. (2008). "Characteristics of particulate carbon emissions from real-world Chinese coal combustion." Environmental Science & Technology **42**(14): 5068-5073.

WEB REFERENCES

http://placesdata.com/world/kyrgyzstan/bishkek/. Accessed March 31, 2011.

http://placesdata.com/world/kyrgyzstan/karakol/ Accessed March 31, 2011.

http://placesdata.com/world/kyrgyzstan/teploklyuchenka/ Accessed March 31, 2011.

http://www.state.gov/r/pa/ei/bgn/5755.htm. Accessed September 10, 2010.

Figure Captions

Figure 1: Map of Central Asia and location of the Aral Sea relative to the Kyrgyz Republic, as well as approximate location of sampling sites within Kyrgyz Republic (inset). See text for coordinates.

Figures 2A-2D: 2A (top left) and 2B (bottom left)-average $PM_{2.5}$ monthly concentrations of elemental carbon (EC), water insoluble organic carbon (WIOC) and water-soluble organic carbon (WSOC) observed at the Bishkek (2A) and LIDAR(2B) sampling sites, respectively. 2C (top right) and 2D (bottom right)-average ratio, on a monthly basis, of OC to total carbon (TC) at Bishkek (2C) and LIDAR (2D) sampling sites.

Figures 3A and 3B: Graphical representation of CMB Source Contribution Estimates for Bishkek (top, 3A) and LIDAR (bottom, 3B) sampling sites.

Figures 4A and 4B: Correlation between non-biomass burning WSOC and sum of CMB "Other" and biogenic SOA at Bishkek site (4A, top) and LIDAR site (4B, bottom). Error bars represent the combination of the propagated analytical uncertainty for the non-biomass burning WSOC combined with the standard error output of the CMB model (x-axis) and the propagated standard error of the CMB "Other" and biogenic SOA SCEs. Because y-intercept of the linear regression equation was not statistically different from zero for both sites, the y-intercept(s) were set equal to zero.

Figures 5A-5D: Comparison of measured $PM_{2.5}$ OC (5A, top left), SOA-Derived $PM_{2.5}$ OC (5B, bottom left), biomass burning $PM_{2.5}$ OC (5C, top right), and mobile-source derived $PM_{2.5}$ OC (5D, bottom right) between Bishkek site (x-axis) and LIDAR site (y-axis). Diagonal lines in all four graphs represent 1/1 lines for reference. Seasonal designations are as follows: "Summer": June, July, August; "Fall": September, October, November; "Winter": December, January, February; "Spring": March, April, May.

Figure SI-1A-SI-1B: $PM_{2.5}$ OC/EC ratios for Bishkek (Top, 1A), and LIDAR (Bottom, 1B) sampling sites, corresponding to Figures 2C and 2D from the main text. The OC/EC ratios plotted represent the ratios of the monthly averages of each quantity.

Figure SI-2: Comparison of low-temperature coal combustion Source Contribution Estimates (SCEs) from Chemical Mass Balance (CMB) modeling analysis between Bishkek and LIDAR sampling sites. Error bars represent the standard error of the SCEs. The absence of a data point for a particular month indicates that the molecular marker critical to that source profile (in this case, picene for low temperature coal combustion) was not present above the detection limit in the GC-MS analysis.

Figure SI-3A-SI-3B: Comparison of $PM_{2.5}$ WIOC (3A), $PM_{2.5}$ WSOC (3B), and $PM_{2.5}$ EC (3C) concentrations between the two sampling sites, Bishkek (x-axis) and LIDAR (y-axis). The data points are coded by sampling season. Seasonal designations are as follows: "Summer": June, July, August; "Fall": September, October, November; "Winter": December, January, February; "Spring": March, April, May.

Figure 1

Figure 1

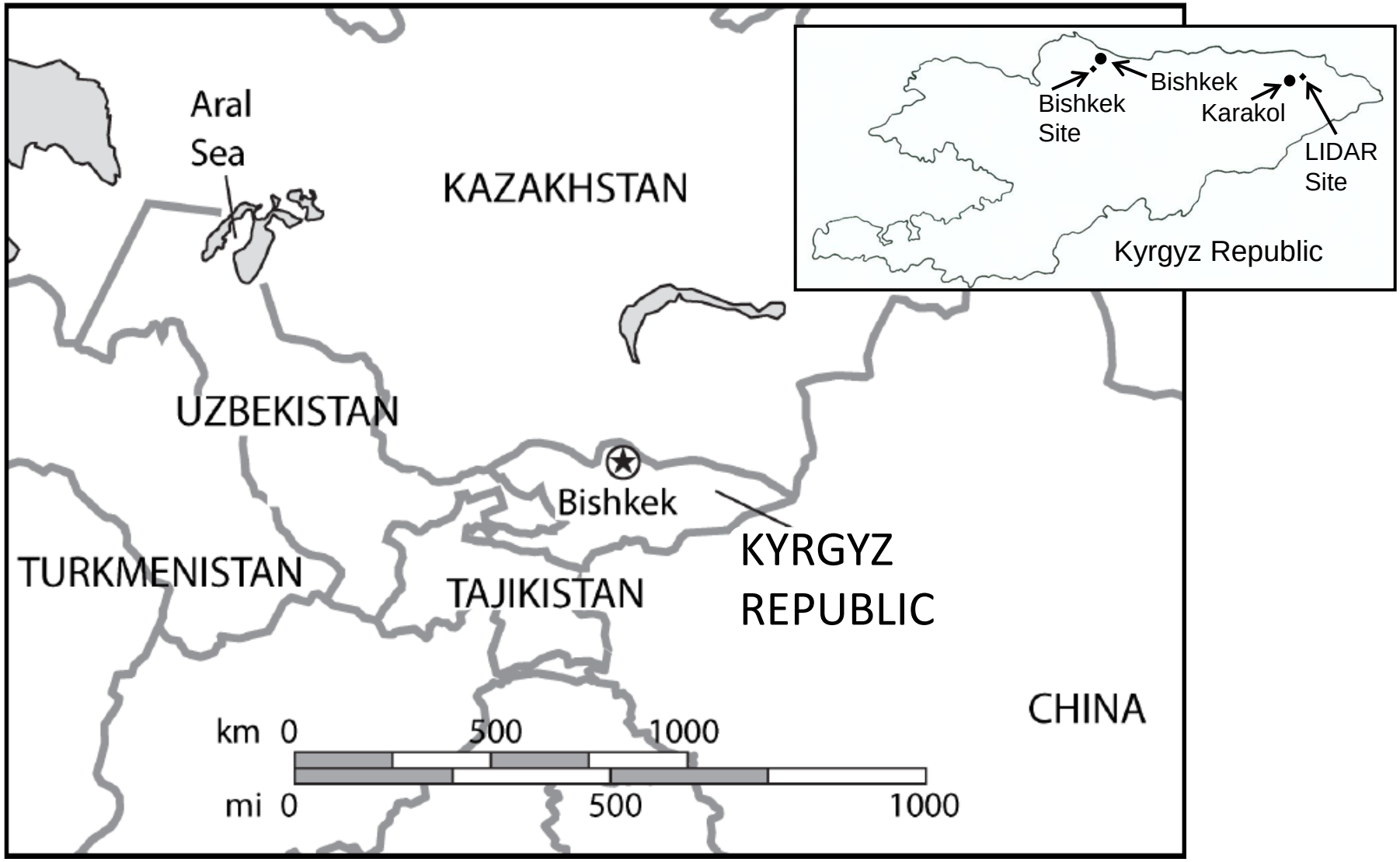

Figure 2A,2B,2C,2D

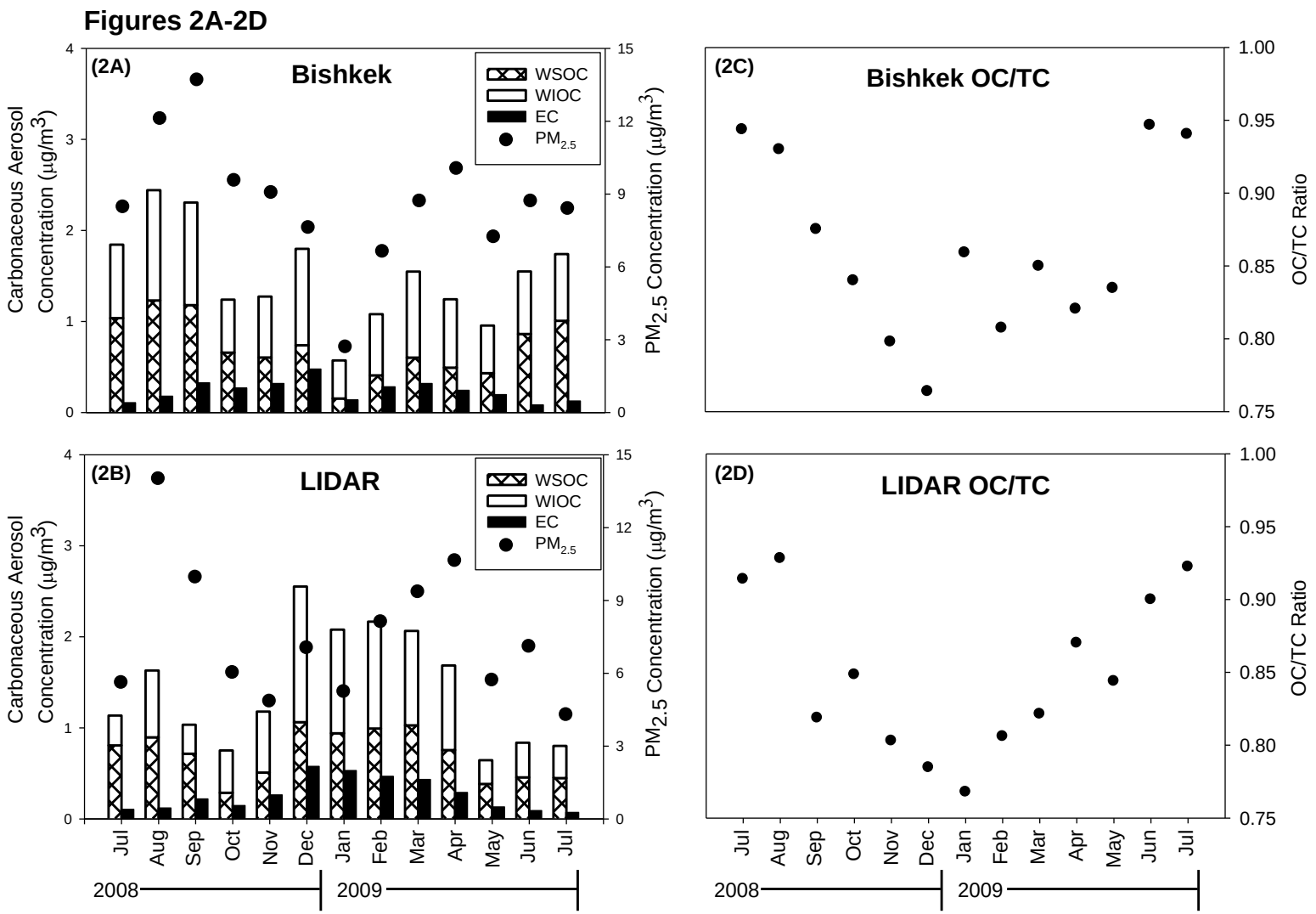

Figure 3A,3B

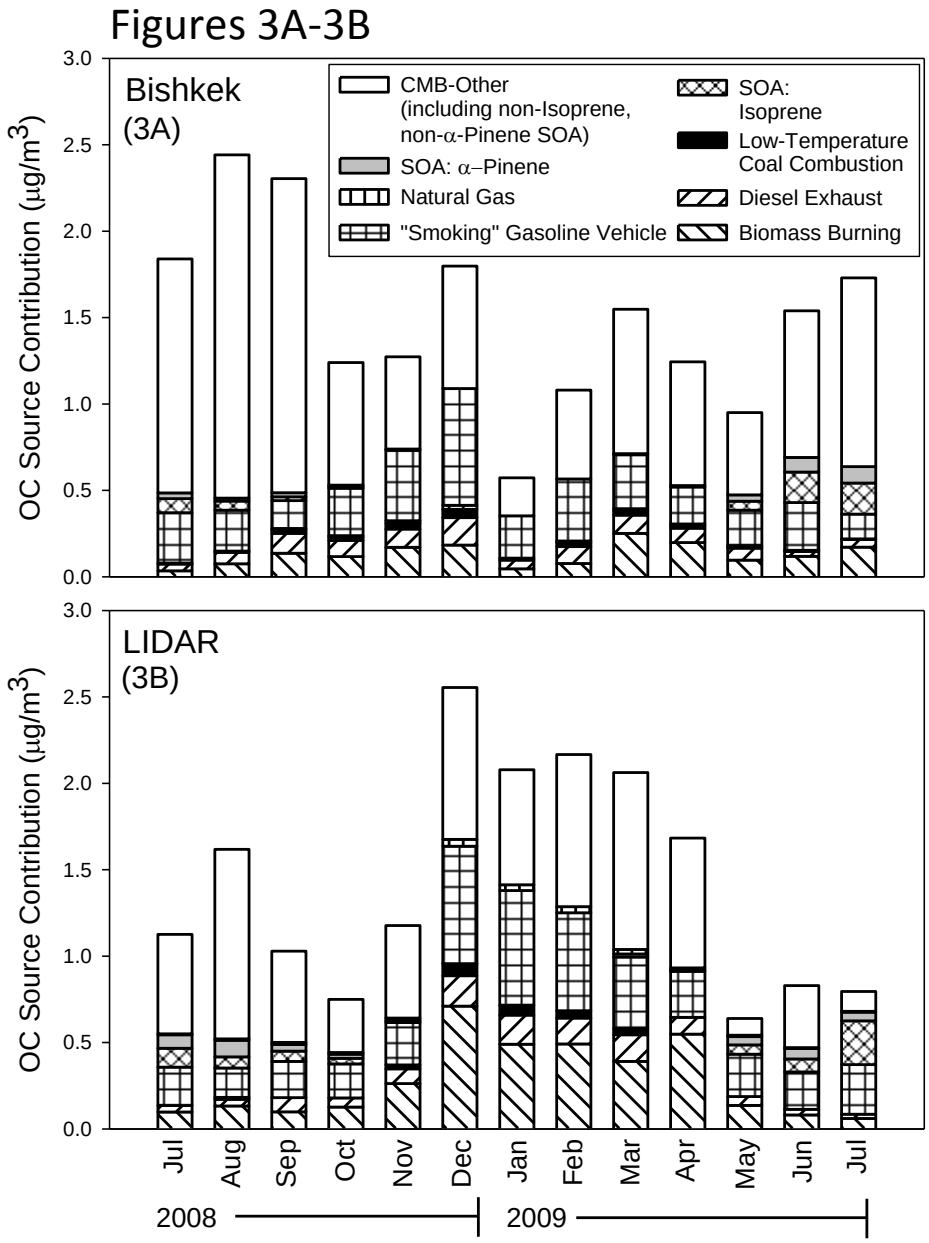
Figures 3A-3B
Bishkek
(3A)
LIDAR
(3B)
OC Source Contribution (μg/m3)
CMB-Other
(including non-Isoprene,
non-α-Pinene SOA)
SOA: α–Pinene
Natural Gas
"Smoking" Gasoline Vehicle
SOA:
Isoprene
Low-Temperature
Coal Combustion
Diesel Exhaust
Biomass Burning
0.0
0.5
1.0
1.5
2.0
2.5
3.0
Jul
Aug
Sep
Oct
Nov
Dec
Jan
Feb
Mar
Apr
May
Jun
Jul
2008
2009

Figure 4A,4B

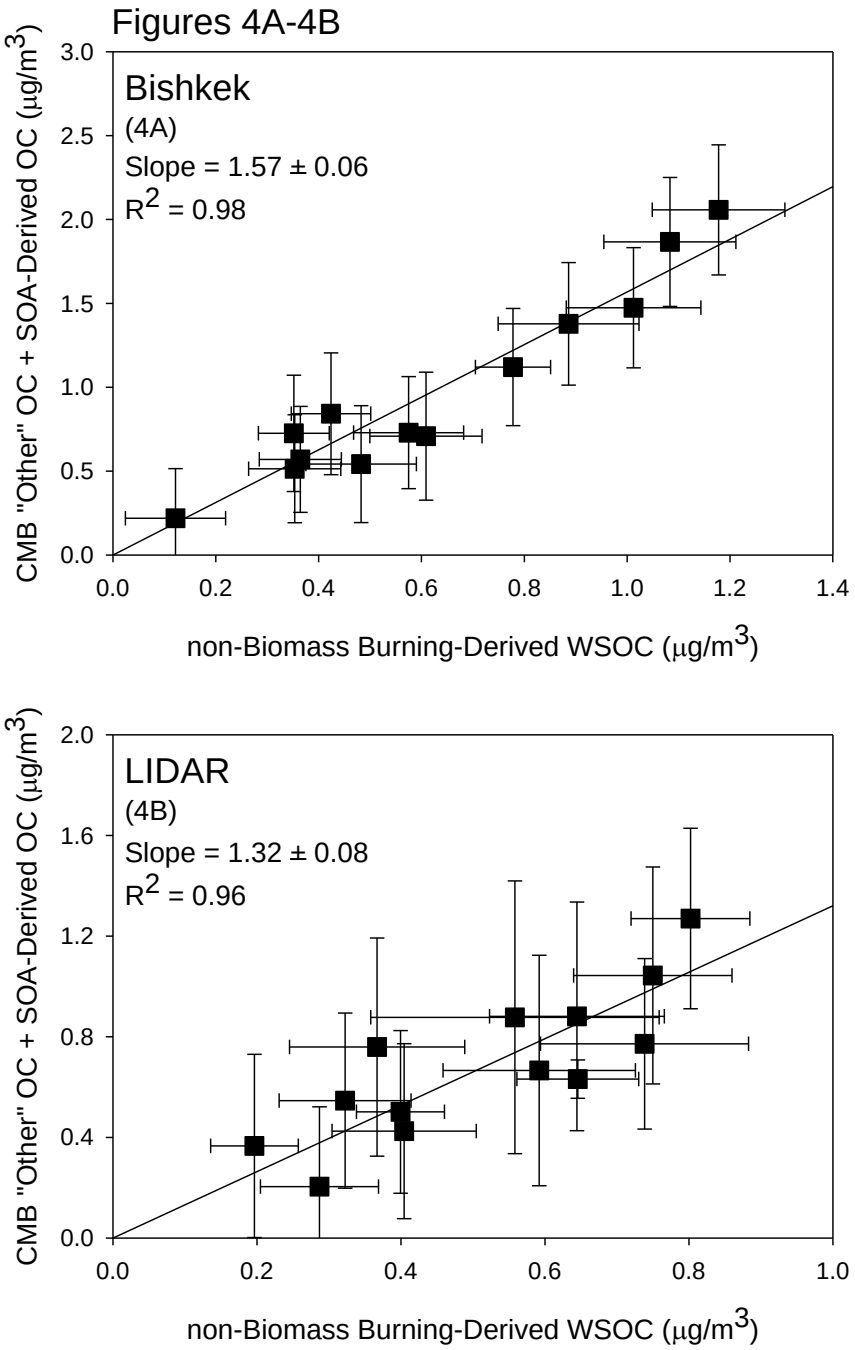
Figures 4A-4B
Bishkek
(4A)
Slope = 1.57 ± 0.06
R2 = 0.98
CMB "Other" OC + SOA-Derived OC (μg/m3)
non-Biomass Burning-Derived WSOC (μg/m3)
0.0
0.5
1.0
1.5
2.0
2.5
3.0
0.0
0.2
0.4
0.6
0.8
1.0
1.2
1.4
LIDAR
(4B)
Slope = 1.32 ± 0.08
R2 = 0.96
CMB "Other" OC + SOA-Derived OC (μg/m3)
non-Biomass Burning-Derived WSOC (μg/m3)
0.0
0.4
0.8
1.2
1.6
2.0
0.0
0.2
0.4
0.6
0.8
1.0

Figure 5A,5B,5C,5D

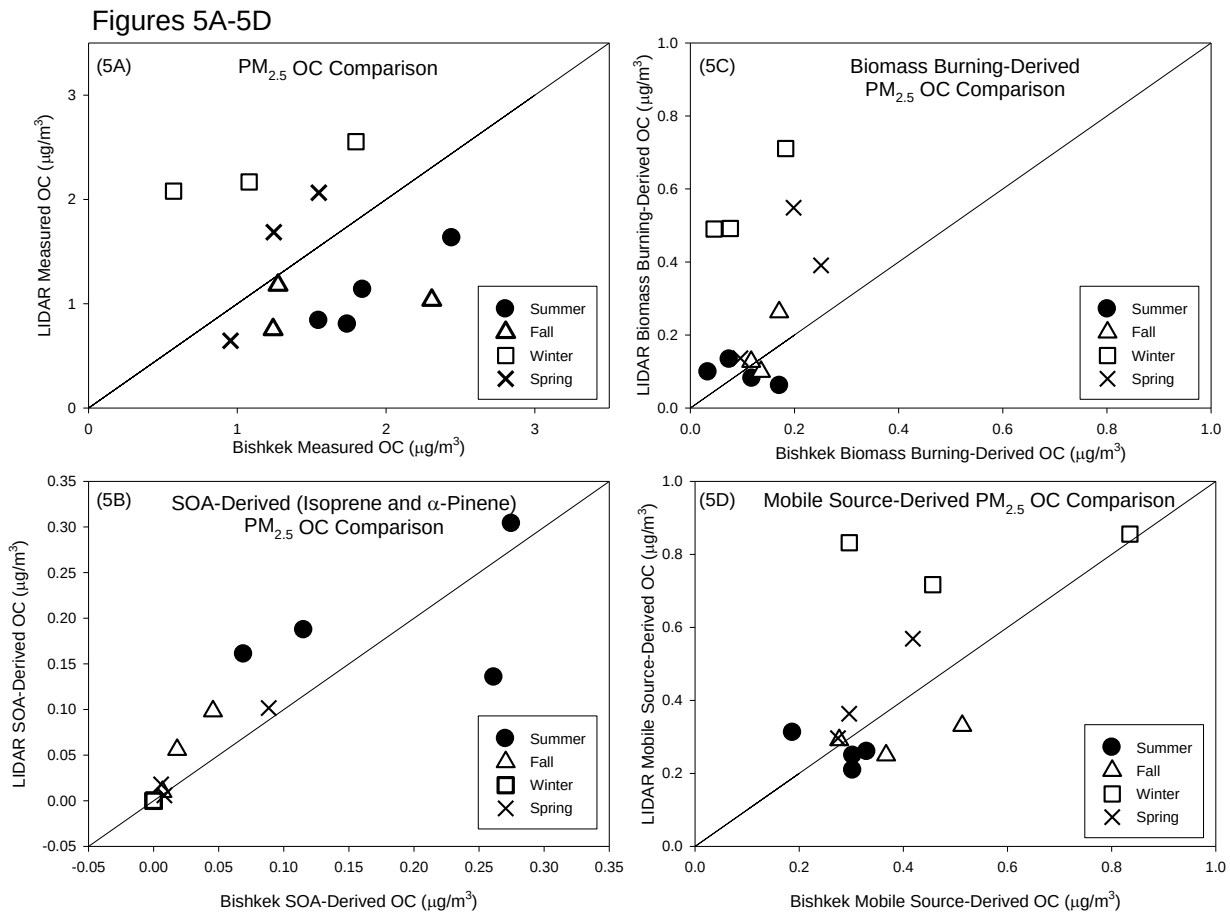

Table 1A

Table 1A: Tracer species used in CMB analysis, minimum and maximum concentration measured in monthly composites, and relevant source profiles for each tracer at the Bishkek site.

BISHKEK			
Tracer Species	Minimum Concentration (pg/m^3)*	Maximum Concentration (pg/m^3)	Source Profile(s)**
Elemental Carbon	7.200×10^4	5.770×10^5	BB, DE, GE, SGE, LTC, NG
Benzo(b)fluoranthene	57.90	343.9	BB, DE, GE, SGE, LTC, NG
Benzo(k)fluoranthene	37.41	382.1	BB, DE, GE, SGE, LTC, NG
Benzo(e)pyrene	35.53	257.0	BB, DE, GE, SGE, LTC, NG
Benzo(a)pyrene	<8.079	129.6	DE, GE, SGE
Perylene	<8.079	41.45	DE, GE, SGE
Picene	<12.12	51.77	LTC
17A(H)-22,29,30-Trisnorhopane	<8.079	83.61	DE, GE, SGE, LTC
17B(H)-21A(H)-30-Norhopane	<4.039	146.5	DE, GE, SGE, LTC
17A(H)-21B(H)-Hopane	23.48	118.9	DE, GE, SGE, LTC
I-2 (2-methylthreitol)	<202.0	1.063×10^4	isoprene SOA
I-3 (2-methylerythreitol)	<202.0	1.752×10^4	isoprene SOA
A-5 (3-hydroxyglutaric acid)	<202.0	4209	α-pinene SOA
PA (pinic acid)	<202.0	2899	α-pinene SOA
A-6 (2-hydroxy-4,4-dimethylglutaric acid)	<202.0	2044	α-pinene SOA
A-4 (3-acetyl hexanedioic acid)	<202.0	4163	α-pinene SOA
A-3 (2-hydroxy-4-ispropyladipic acid)	<202.0	3700	α-pinene SOA
Levoglucosan	3209	2.378×10^4	BB, LTC

***: If minimum values include a "<", this indicates that the minimum value was calculated to be less than the method limit-of-detection for that analyte**

****: Source Profile Abbreviations (Reference in Parentheses):**

BB: Biomass Burning (Lee, Baumann et al. 2005)

DE: Diesel Exhaust (Lough, Christensen et al. 2007)

GE: Gasoline Engines (Lough, Christensen et al. 2007)

SGV: Smoking Gasoline Vehicles (Lough, Christensen et al. 2007)

LTC: Low Temperature Coal Combustion ((Zhang, Schauer et al. 2008)

NG: Natural Gas ((Rogge, Hildemann et al. 1993)

Isoprene SOA: isoprene-derived SOA (Lewandowski, Jaoui et al. 2007)

α-pinene SOA: α-pinene-derived SOA (Lewandowski, Jaoui et al. 2007)

Table 1B

Table 1B: Tracer species used in CMB analysis, minimum and maximum concentration measured in monthly composites, and relevant source profiles for each tracer at the LIDAR site.

LIDAR			
Tracer Species	Minimum Concentration (pg/m^3)*	Maximum Concentration (pg/m^3)	Source Profile(s)**
Elemental Carbon	8.400×10^4	4.780×10^5	BB, DE, GE, SGE, LTC, NG
Benzo(b)fluoranthene	70.53	566.0	BB, DE, GE, SGE, LTC, NG
Benzo(k)fluoranthene	46.42	586.3	BB, DE, GE, SGE, LTC, NG
Benzo(e)pyrene	<12.58	462.5	BB, DE, GE, SGE, LTC, NG
Benzo(a)pyrene	<8.384	338.2	DE, GE, SGE
Perylene	<8.384	71.97	DE, GE, SGE
Picene	<12.58	69.63	LTC
17A(H)-22,29,30-Trisnorhopane	<8.384	74.44	DE, GE, SGE, LTC
17B(H)-21A(H)-30-Norhopane	6.922	136.6	DE, GE, SGE, LTC
17A(H)-21B(H)-Hopane	30.86	113.2	DE, GE, SGE, LTC
I-2 (2-methylthreitol)	<209.6	1.664×10^5	isoprene SOA
I-3 (2-methylthreitol)	<209.6	2.258×10^5	isoprene SOA
A-5 (3-hydroxyglutaric acid)	<209.6	1594	α-pinene SOA
PA (pinic acid)	<209.6	3856	α-pinene SOA
A-6 (2-hydroxy-4,4-dimethylglutaric acid)	<209.6	732.3	α-pinene SOA
A-4 (3-acetyl hexanedioic acid)	<209.6	6023	α-pinene SOA
A-3 (2-hydroxy-4-ispropyladipic acid)	<209.6	1402	α-pinene SOA
Levoglucosan	5765	6.554×10^5	BB, LTC

***: If minimum values include a "<", this indicates that the minimum value was calculated to be less than the method limit-of-detection for that analyte**

****: Source Profile Abbreviations (Reference in Parentheses):**
BB: Biomass Burning (Lee, Baumann et al. 2005)
DE: Diesel Exhaust (Lough, Christensen et al. 2007)
GE: Gasoline Engines (Lough, Christensen et al. 2007)
SGV: Smoking Gasoline Vehicles (Lough, Christensen et al. 2007)
LTC: Low Temperature Coal Combustion ((Zhang, Schauer et al. 2008)
NG: Natural Gas ((Rogge, Hildemann et al. 1993)
Isoprene SOA: isoprene-derived SOA (Lewandowski, Jaoui et al. 2007)
α-pinene SOA: α-pinene-derived SOA (Lewandowski, Jaoui et al. 2007)

Table 2

Click here to download Table: Table 2.ppt

Table 2: Monthly averages of $PM_{2.5}$ concentrations, $PM_{2.5}$ OC, and % of $PM_{2.5}$ as OC observed at both sampling sites for the duration of the study.

	Bishkek						LIDAR					
Month /Year	$PM_{2.5}$	Std Err* (µg/m3)	OC in $PM_{2.5}$	Std Err (µg/m3)	% $PM_{2.5}$ as OC	Std Err	$PM_{2.5}$	Std Err (µg/m3)	OC in $PM_{2.5}$	Std Err (µg/m3)	% $PM_{2.5}$ as OC	Std Err
Jul/2008	8.46	0.88	1.84	0.18	22	1.4	5.60	0.38	1.14	0.07	20	8.0
Aug/2008	12.1	0.65	2.44	0.14	21	1.2	14.0	3.00	1.63	0.18	14	1.6
Sep/2008	13.7	0.83	2.31	0.19	17	0.94	9.95	0.96	1.03	0.12	11	0.93
Oct/2008	9.55	1.69	1.24	0.16	16	1.8	6.02	0.52	0.75	0.10	12	1.2
Nov/2008	9.05	1.85	1.27	0.29	15	1.0	4.84	0.64	1.18	0.20	24	2.6
Dec/2008	7.61	1.31	1.80	0.33	23	1.4	7.04	0.89	2.55	0.54	33	2.6
Jan/2009	2.69	0.50	0.57	0.12	20	1.6	5.23	0.56	2.08	0.30	38	3.3
Feb/2009	6.62	0.81	1.08	0.14	17	1.7	8.11	0.84	2.17	0.32	26	2.3
Mar/2009	8.70	1.36	1.55	0.26	20	0.0	9.34	1.28	2.06	0.30	23	1.9
Apr/2009	10.0	2.13	1.27	0.21	12	1.4	10.6	1.59	1.69	0.31	19	2.9
May/2009	7.22	0.85	0.96	0.18	13	1.5	5.70	1.01	0.64	0.14	11	1.4
Jun/2009	7.82	0.47	1.55	0.14	20	1.7	7.10	1.71	0.84	0.07	14	1.6
Jul/2009	8.39	0.42	1.74	0.17	21	0.2	4.28	1.02	0.80	0.14	21	3.0

*:The uncertainty given represents the standard error for the data for that month, i.e., the standard deviation of the monthly data divided by the square root of the number of measurements in that month.

Table 3
Click here to download Table: Table 3.doc

Table 3: Source Contribution Estimates (SCEs) from Chemical Mass Balance modeling analysis for the Bishkek sampling site. "Mobile Sources" represents the sum of the diesel and gasoline engine emission SCEs, and "Biogenic SOA" represents the sum of the α-pinene- and isoprene-derived SOA SCEs. CMB "Other" represents the difference between the measured (monthly average) OC and the sum of the SCEs for the identified sources in Table 3. See text for details.

Bishkek								
Month/ Year	Measured OC ($\mu g/m^3$)	Biomass Combustion ($\mu g/m^3$)	Natural Gas Combustion ($\mu g/m^3$)	Low-Temperature Coal Combustion* ($\mu g/m^3$)	Mobile Sources ($\mu g/m^3$)	Biogenic SOA ($\mu g/m^3$)	% Mass Apportioned	CMB "Other" ($\mu g/m^3$)
Jul/08	1.84	0.034	0.006	N.D.	0.330	0.115	26.3	1.36
Aug/08	2.44	0.075	0.007	N.D.	0.303	0.069	18.6	1.99
Sep/08	2.31	0.136	0.009	0.019	0.277	0.046	21.1	1.82
Oct/08	1.24	0.117	0.010	0.017	0.367	0.018	42.7	0.711
Nov/08	1.27	0.171	0.016	0.032	0.513	0.007	58.0	0.535
Dec/08	1.80	0.183	0.024	0.048	0.835	N.D.	60.6	0.709
Jan/09	0.572	0.046	0.011	N.D.	0.296	N.D.	61.7	0.219
Feb/09	1.08	0.077	0.010	0.022	0.456	N.D.	52.4	0.514
Mar/09	1.55	0.251	0.011	0.026	0.418	0.006	46.0	0.836
Apr/09	1.24	0.198	0.010	0.015	0.296	0.008	42.4	0.717
May/09	0.955	0.096	0.006	0.009	0.274	0.088	49.6	0.481
Jun/09	1.55	0.119	0.007	N.D.	0.303	0.261	44.6	0.859
Jul/09	1.74	0.172	0.004	N.D.	0.188	0.275	36.6	1.10

***: "N.D." indicates that the molecular marker critical to this source profile was not present above the detection limit.**

Table 4
Click here to download Table: Table 4.doc

Table 4: Source Contribution Estimates (SCEs) from Chemical Mass Balance modeling analysis for the LIDAR sampling site. "Mobile Sources" represents the sum of the diesel and gasoline engine emission SCEs, and "Biogenic SOA" represents the sum of the α-pinene- and isoprene-derived SOA SCEs. CMB "Other" represents the difference between the measured (monthly average) OC and the sum of the SCEs for the identified sources in Table 4. See text for details.

LIDAR								
Month/ Year	Measured OC ($\mu g/m^3$)	Biomass Combustion ($\mu g/m^3$)	Natural Gas Combustion ($\mu g/m^3$)	Low-Temperature Coal Combustion* ($\mu g/m^3$)	Mobile Sources ($\mu g/m^3$)	Biogenic SOA ($\mu g/m^3$)	% Mass Apportioned	CMB "Other" ($\mu g/m^3$)
Jul/08	1.14	0.098	0.006	N.D.	0.259	0.187	48.5	0.585
Aug/08	1.63	0.133	0.008	0.011	0.208	0.161	32.0	1.11
Sep/08	1.03	0.099	0.012	N.D.	0.291	0.098	48.4	0.533
Oct/08	0.752	0.127	0.009	N.D.	0.250	0.056	58.8	0.310
Nov/08	1.18	0.262	0.016	0.022	0.330	0.010	54.5	0.536
Dec/08	2.55	0.711	0.040	0.069	0.855	N.D.	65.6	0.877
Jan/09	2.80	0.490	0.034	0.057	0.832	N.D.	68.0	0.666
Feb/09	2.17	0.492	0.035	0.042	0.717	N.D.	59.3	0.881
Mar/09	2.06	0.390	0.026	0.035	0.569	0.018	50.3	1.03
Apr/09	1.68	0.548	0.014	N.D.	0.363	0.006	55.3	0.753
May/09	0.645	0.136	0.008	N.D.	0.296	0.102	84.1	0.102
Jun/09	0.837	0.081	0.006	N.D.	0.249	0.135	56.3	0.366
Jul/09	0.802	0.061	0.005	N.D.	0.312	0.304	84.9	0.121

*** "N.D." indicates that the molecular marker critical to this source profile was not present above the detection limit.**

Supporting Information

Click here to download e-component: Supporting Information.doc

Figure SI-1A,SI-1B

Click here to download e-component: Figure SI-1A_SI-1B.doc

Figure SI-2

Click here to download e-component: Figure SI-2.doc

Figure SI-3A,SI-3B,SI-3C

Click here to download e-component: Figure SI-3A_SI-3B_SI-3C.doc

Table SI-1

Click here to download e-component: Table SI-1.doc

Table SI-2A

Click here to download e-component: Table SI-2A.doc

Table SI-2B

Click here to download e-component: Table SI-2B.doc

Table SI-3A

Click here to download e-component: Table SI-3A.doc

Table SI-3B

Click here to download e-component: Table SI-3B.doc